4318 *Biochemistry* **1989**, *28*, 4318–4325

Nucleotide and AP_5A Complexes of Porcine Adenylate Kinase: A ^1H and ^{19}F NMR Study

Paul Rösch,* Werner Klaus,‡ Manfred Auer, and Roger S. Goody

Department of Biophysics, Max Planck Institute for Medical Research, Jahnstrasse 29, D-6900 Heidelberg 1, FRG

Received July 18, 1988; Revised Manuscript Received January 30, 1989

ABSTRACT: Proton and fluorine nuclear magnetic resonance spectroscopies (NMR) were used as methods to investigate binary complexes between porcine adenylate kinase (AK_1) and its substrates. We also studied the interaction of fluorinated substrate analogues and the supposed bisubstrate analogue P^1,P^5-bis(5′-adenosyl) pentaphosphate (AP_5A) with AK_1 in the presence of Mg^{2+}. The chemical shifts of the C8-H, C2-H, and ribose C1′-H resonances of both adenosine units in stoichiometric complexes of AK_1 with AP_5A in the presence of Mg^{2+} could be determined. The C2-H resonance of one of the adenine bases experiences a downfield shift of about 0.8 ppm on binding to the enzyme. The chemical shift of the His^{36} imidazole C2-H was changed in the downfield direction on $ATP{\cdot}Mg^{2+}$ and, to a lesser extent, AMP binding. ^{19}F NMR chemical shifts of 9-(3-fluoro-3-deoxy-β-D-xylofuranosyl)adenine triphosphate (3′-F-X-ATP)–Mg^{2+} and 9-(3-fluoro-3-deoxy-β-D-xylofuranosyl)adenine monophosphate (3′-F-X-AMP) bound to porcine adenylate kinase could be determined. The different chemical shifts of the bound nucleotides suggest that their mode of binding is different. Free and bound 3′-F-X-AMP are in fast exchange with respect to their ^{19}F chemical shifts, whereas free and bound 3′-F-X-ATP are in slow exchange on the NMR time scale in the absence as well as in the presence of Mg^{2+}. This information could be used to determine the apparent dissociation constants of the nucleotides and the 3′-F-X analogues in the binary complexes. A strong nuclear Overhauser effect (NOE) could be detected between one of the two C2 protons of AP_5A and the C2 proton of the imidazole ring of His^{36}. This proton thus belongs to the site which was earlier suggested to be the $ATP{\cdot}Mg^{2+}$ site for the pig as well as for the rabbit enzyme (Smith & Mildvan, 1983; Fry et al., 1985, 1988).

Adenylate kinases form a family of low molecular weight phosphokinases. The porcine cytosolic adenylate kinase (AK_1, myokinase, ATP:AMP phosphotransferase, EC 2.7.4.3),[1] with a molecular mass of 21.7 kDa is the smallest phosphokinase known (Noda, 1971). It catalyzes the transfer of a phosphoryl group between ATP and AMP in the presence of a divalent cation, physiologically Mg^{2+}, according to

$$\mathrm{ATP{\cdot}Mg^{2+} + AMP \underset{k_{-1}}{\overset{k_1}{\rightleftharpoons}} ADP{\cdot}Mg^{2+} + ADP}$$

As suggested by the catalyzed reaction, AK_1 possesses two nucleotide binding sites, one for the metal-complexed nucleotide ($ATP{\cdot}Mg^{2+}$, acceptor $ADP{\cdot}Mg^{2+}$) and one for the metal-free nucleotide (donor ADP, AMP), corresponding to a phosphoryl-donor and a phosphoryl-acceptor site. The tertiary structure of the substrate-free porcine AK_1 is known (Schulz et al., 1974), and the primary structures of several other adenylate kinases were determined in recent years [see Schulz et al. (1986) and literature cited therein]. The location of the two nucleotide binding sites is still under debate since no conclusive X-ray structure of a complex of nucleotides and any of the adenylate kinases is known.

Much effort has been invested in studies aimed at localizing the nucleotide binding sites of porcine adenylate kinase and other adenylate kinases, e.g., the rabbit, yeast (AK_y), or *Escherichia coli* (AK_{EC}) enzymes. Porcine AK_1 does not cocrystallize with either or both of its substrates or the supposed bisubstrate analogue P^1,P^5-bis(5′-adenosyl) pentaphosphate (AP_5A). The crystal structures of the complexes of AK_y with $AP_5A{\cdot}Mg^{2+}$ and AK_{EC} with $AP_5A{\cdot}Mg^{2+}$ were determined only recently (Egner et al., 1987; Müller & Schulz, 1988). Egner et al. (1987) cautioned that the $AK_y{\cdot}AP_5A{\cdot}Mg^{2+}$ crystal structure does not necessarily reflect both binding sites, but the similarity of this structure with the $AK_{EC}{\cdot}AP_5A$ crystal structure added confidence to the assumption that the $AP_5A{\cdot}Mg^{2+}$ complex occupies both nucleotide sites. Proton NMR studies attempting to measure nuclear Overhauser effects from the porcine protein to AMP or ATP in the presence of excess nucleotide and exploitation of paramagnetic effects on the NMR spectrum lead to the suggestion of a localization of the $ATP{\cdot}Mg^{2+}$ binding site near His^{36} (McDonald et al., 1975; Smith & Mildvan, 1982). The imidazole C2 proton of His^{36} was found to be very close to the adenine C2 proton of $ATP{\cdot}Mg^{2+}$. This result was corroborated by investigation of synthetic peptides supposed to represent the nucleotide binding sites of AK_1 (Hamada et al., 1979; Fry et al., 1985, 1988).

The results obtained from the X-ray studies of $AK_y{\cdot}AP_5A{\cdot}Mg^{2+}$ and $AK_{EC}{\cdot}AP_5A{\cdot}Mg^{2+}$ crystals were virtually identical (Egner et al., 1987; Müller & Schulz, 1988). These results and early X-ray studies with porcine AK_1 crystals with incorporated salicylate (Pai et al., 1975) are not reconcilable

---

‡ W.K. was supported by grants from the Deutsche Forschungsgemeinschaft (Ro 617/1-1 and Ro 617/1-2). Present address: Department of Molecular Structure Research, GBF, Mascherodeweg 1, D-3300 Braunschweig, FRG.

[1] Abbreviations: AK, adenylate kinase; ADP, adenosine 5′-diphosphate; AMP, adenosine 5′-monophosphate; AP_4A, P^1,P^4-bis(5′-adenosyl) tetraphosphate; AP_5A, P^1,P^5-bis(5′-adenosyl) pentaphosphate; AP_6A, P^1,P^6-bis(5′-adenosyl) hexaphosphate; ATP, adenosine 5′-triphosphate; δ_b, chemical shift in the bound state; δ_f, chemical shift in the free state; DSS, sodium 4,4-dimethyl-4-silapentanesulfonate; DTE, dithioerythritol; 3′-F-X-AMP, 9-(3-fluoro-3-deoxy-β-D-xylofuranosyl)adenine monophosphate; 3′-F-X-ATP, 9-(3-fluoro-3-deoxy-β-D-xylofuranosyl)adenine triphosphate; K_d dissociation constant; NMR, nuclear magnetic resonance; NOE, nuclear Overhauser effect; NOESY, nuclear Overhauser enhancement spectroscopy; Hepes, N-(2-hydroxyethyl)piperazine-N'-2-ethanesulfonic acid; tris(hydroxymethyl)aminomethane.

0006-2960/89/0428-4318$01.50/0

with each other and with the NMR results. Previous NMR studies aimed at the localization of the nucleotide binding sites and the study of adenylate kinase–nucleotide complexes were criticized mainly for two reasons: first, resonance assignments were restricted to the knowledge of the imidazole C2 protons of His^{36} and His^{189} in porcine adenylate kinase; second, the experiments were performed at high excess of substrate (e.g., 10-fold) over protein or with synthetic peptides, both methods giving only indirect clues.

In order to circumvent at least some of these problems, we conducted ^1H NMR studies of samples with stoichiometric amounts of nucleotides and enzyme. We recently suggested assignments for the aromatic side-chain resonances of the porcine adenylate kinase (Klaus et al., 1988). The question whether the mono-, di-, or triphosphates may occupy both binding sites on the enzyme was approached earlier with a variety of methods [e.g., Hamada et al. (1979), Shyy et al. (1987), and Nageswara Rao et al. (1978)], and kinetic studies indicated that at least $AMP{\cdot}Mg^{2+}$—if not magnesium-free AMP—can bind to the triphosphate site (Rhoades & Lowenstein, 1968).

MATERIALS AND METHODS

Porcine adenylate kinase was prepared and activity measured essentially as described earlier (Barzu & Michelson, 1983; Berghäuser & Schirmer, 1978). The protein was stored as a lyophilized powder at 253 K after the preparation. The nucleotide content of all protein samples was checked by HPLC before use; the nucleotide concentration was found to be less than 2% of the protein concentration in all cases (in most cases the level of nucleotide present was below the limits of detection). In addition, after all experiments involving nucleotides, the nucleotide composition in the samples was checked by HPLC; over 95% of the nucleotide concentration stated in the description of the experiments was still present after the experiments in all cases. An exception was the stoichiometric complexes of adenylate kinase with $ATP{\cdot}Mg^{2+}$ at elevated temperature, since the half-life of the nucleotide under these conditions was only of the order of several hours.

For NMR experiments, residual H_2O was exchanged for D_2O by addition of D_2O (99.8% from Sigma) to a preweighed amount of protein, followed by overnight storage at room temperature in order to exchange labile amide protons. Then the protein was lyophilized and subsequently dissolved in D_2O ("100%" from Sigma) to the desired concentration. Protein concentration was determined before the NMR experiments according to Ehresman et al. (1973). Nucleotides were obtained from Sigma at the highest purity commercially available. Fluorine nucleotides (3′-F-X-AMP and 3′-F-X-ATP) were prepared as described elsewhere (Auer et al., 1988). AP_5A was prepared according to Feldhaus et al. (1975). Final buffer concentration was about 50 mM Hepes; DTE was present in all solutions in a concentration approximately equimolar with the protein concentration. pH values were adjusted with NaOD and DCl if necessary. Reported values represent direct meter readings without correction for the deuterium isotope effect.

NMR experiments were performed on a commercial Bruker AM 500 spectrometer operating at a proton resonance frequency of 500 MHz. For two-dimensional NMR experiments we used approximately 2.5 mM solutions; the one-dimensional experiments were performed generally with less than 1 mM solutions. The sample was kept at the desired temperature with a precooled stream of dry air, temperature regulated with a standard Bruker VT 1000 unit. The residual HDO resonance was suppressed by permanent (except acquisition) selective irradiation with the HDO frequency. Quadrature detection was used in all experiments. Standard procedures and commercially available software were used throughout. Sample tubes of 5 mm were used for all proton NMR experiments and 10-mm sample tubes for the fluorine NMR experiments. All proton NMR spectra were referenced to internal sodium 4,4-dimethyl-4-silapentanesulfonate (DSS); fluorine spectra were referenced to external trifluoroacetic acid.

NOE experiments were performed under the same conditions as the other 1D experiments except for the introduction of a relaxation delay of 1.2 s and an irradiation time period of 1 s before data collection. This gave a total pulse spacing of approximately 3.8 s. The NOE data were collected as usual according to the scheme: $(\{[RD–IR(\omega_i)–DS]_4–[RD–IR(\omega_i)–AQ]_{32}\}_i)_n$, where $i = 1$ or 2 ($i = 1$, on-resonance irradiation; $i = 2$, off-resonance irradiation in a resonance-free region of the spectrum), RD = 1.2 s, DS = dummy scans without data collection, IR = irradiation of the frequency i, AQ = data acquisition, and n = number of repetitions of the sequence, between 40 and 50, leading to the overnight accumulation of 1280–1600 scans per experiment. Most NOE experiments were performed at two different temperatures, namely, 283 and 303 K. The qualitative results of both sets of experiments were identical.

Two-dimensional NMR experiments were performed in phase-sensitive mode with quadrature detection in both dimension with the time proportional incrementation (TPPI) method (Marion & Wüthrich, 1983).

Apparent dissociation constants for the case of fast two-site exchange between free and bound substrates were determined with a SIMPLEX least-squares fit of the observed chemical shift δ, the chemical shift in the bound state δ_b, the chemical shift in the free state δ_f, and the dissociation constant K_d to

$$\delta = \frac{1}{2[S]}\left([S] + [E] + K_d - \sqrt{([S] + [E] + K_d)^2 - 4[S][E]}\right)(\delta_b - \delta_f) + \delta_f \quad (1)$$

where [S] is the substrate concentration and [E] is the enzyme concentration. The formula follows easily from the definition of K_d ($K_d = [S_f][E_f]/[ES]$), and, in the fast exchange limit, $\delta = p_b\delta_b + p_f\delta_f$, where p_b and p_f are the relative concentrations of the bound and free substrate, respectively.

RESULTS

$AK_1{\cdot}AMP$ Complex. The spectral region of the aromatic amino acid residues of porcine AK_1 is very well resolved, and suggestions for the assignment of all resonances have been given recently (Figure 1; Klaus et al., 1988). The binary complex of porcine AK_1 with AMP forms on addition of AMP to the protein with a dissociation constant of approximately 10^{-4} M according to Hamada et al. (1979). On successive addition of substoichiometric amounts of nucleotide to a solution of AK_1, the proton NMR spectrum undergoes specific changes related to the formation of the binary complex (Figure 2). In particular, it can be seen easily that in the completely enzyme-bound form of AMP the chemical shifts of the adenine C2-H and adenine C8-H resonances are interchanged as compared to those of the free nucleotide. In fact, the adenine C2-H is shifted downfield in the bound form as compared to the resonance from the free form, whereas the adenine C8-H resonance is virtually unshifted on binding to the enzyme. As can be seen from the changing chemical shift of these two resonances on further addition of AMP, the resonances of the free and bound forms are in the fast-exchange regime of the NMR time scale. The same is true for the His^{36} imidazole

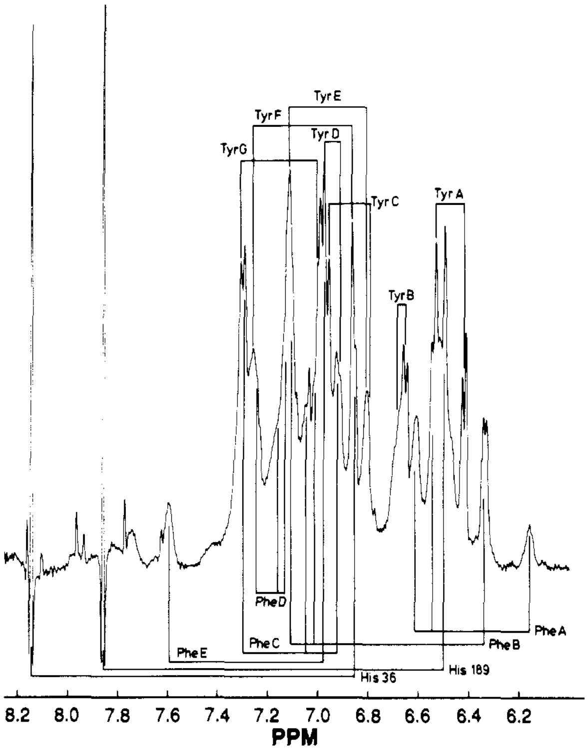

FIGURE 1: Region of the aromatic proton resonances of porcine adenylate kinase with the connectivities as determined by Klaus et al. (1988). Experimental conditions: $T = 303$ K; [AK] = 2.0 mM; phosphate buffer, 50 mM, pH 6.3; FID multiplied by e^{a-bt}, $a = 0.15$ and $b = -10$.

C2-H resonances of the complexed and the uncomplexed forms. On addition of AMP the imidazole C2-H of His^{36} changes its chemical shift in the downfield direction by about 0.04 ppm ($\delta_f = 7.82$ ppm; $\delta_b \approx 7.86$ ppm) to a complete overlap with the His^{189} imidazole C2-H in the presence of a 3-fold excess of AMP over enzyme. Also, the upfield shift of the ring C4-H of Phe^A can be followed easily ($\delta_f = 6.11$ ppm; $\delta_b \approx 5.97$ ppm). An apparent dissociation constant and the chemical shift extrapolated to the completely bound and completely free substrates may be obtained for the adenine C2-H from eq 1 as $\delta_b = 8.68$ ppm, $\delta_f = 8.2$ ppm, and $K_d = 6.1 \times 10^{-5}$ M. Thus, the off-rate for AMP (k_{off}) can be estimated to be much greater than 250 s^{-1}. Addition of $MgCl_2$ did not alter the NMR spectrum. Repetition of the titration of AK_1 with AMP in the presence of a 5-fold excess of $MgCl_2$ did not alter any of the results. This is in accord with the earlier suggestion [Hamada et al. (1979) and literature cited therein] that AMP does not bind as the metal complex.

AK_1·ATP·Mg^{2+} Complex. In contrast to the effect observed in the AK_1·AMP complex, an interchange of chemical shifts of the base protons of ATP in the AK_1·ATP·Mg^{2+} complex could not be observed; in fact, the base protons of the adenine ring are only visible at an approximately 5-fold excess of substrate over protein (Figure 3). As in the nucleoside monophosphate complex, a downfield shift of the imidazole C2-H of His^{36} could be observed, but in this case was larger to the extent that the His^{36} resonance was downfield from the His^{189} resonance in the fully saturated state of the enzyme, $\delta_b = 7.62$ ppm and $\delta_f = 7.52$ ppm. From the chemical shift difference and the fact that the imidazole C2-H resonances of the complexed and uncomplexed protein are in the intermediate- to fast-exchange limit, the off-rate can be estimated to be much greater than 500 s^{-1}. Qualitatively, the rearrangement of the spectrum in the aromatic part was somewhat more pronounced in the AK_1·ATP·Mg^{2+} complex than it was in the AK_1·AMP complex as compared to that of the nucleotide-free enzyme.

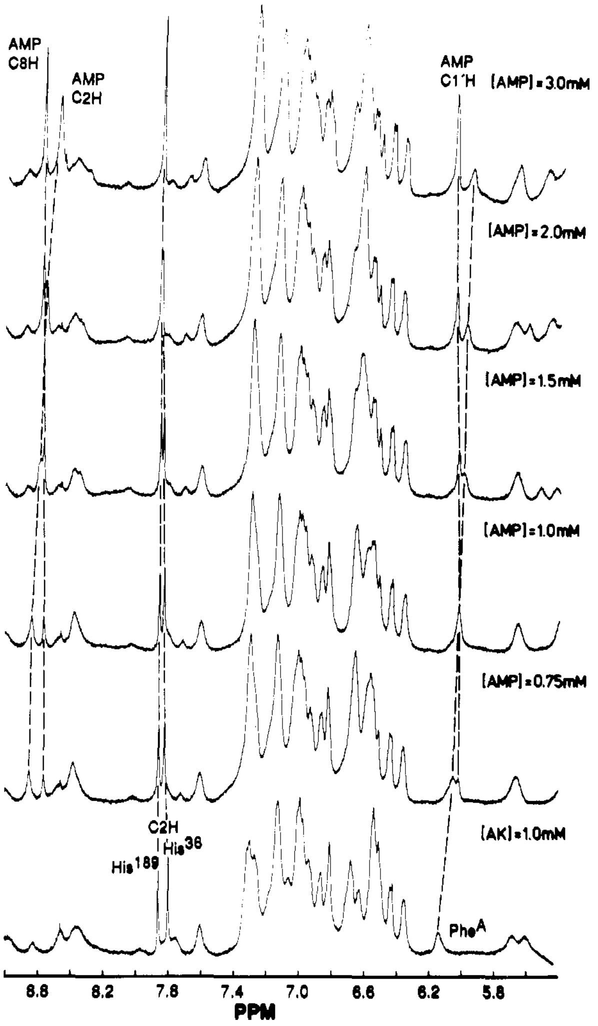

FIGURE 2: Region of the aromatic proton resonances of porcine adenylate kinase and the adenine C2-H and C8-H and the ribose C1′-H resonances at varying AMP nucleotide concentrations. Experimental conditions: $T = 303$ K; Hepes buffer, 50 mM, pH 8.0; concentrations as indicated in the figure.

Details of this rearrangement cannot be followed easily during the titration due to the severe overlap of resonances. One of the resonances which can be traced is the C4-H of the aromatic ring of Phe^A. This resonance is shifted in the opposite direction as in the AK_1·AMP complex, i.e., downfield.

AK·AP_5A·Mg^{2+} Complex. Binding of AP_5A to porcine adenylate kinase induces major changes in the protein structure as shown by changes in the aromatic region of the protein spectrum on AP_5A titration in the presence of $MgCl_2$ (Figure 4) (Kalbitzer et al., 1982). We found that adenylate kinase binds the substrate analogue in a 1:1 ratio as expected from earlier binding studies (Feldhaus et al., 1975). Although it is not possible to follow the spectral changes on AP_5A binding in full detail, some of the assigned resonances alter their chemical shift in an obvious way: For example, the His^{36} imidazole C2-H resonances of the complex at $\delta_b = 8.3$ ppm (for the assignment, see below) and the AP_5A-free AK_1 at $\delta_f = 7.85$ ppm are in slow exchange. Even the C2-H resonances of His^{189} in the complex at $\delta_b = 7.876$ ppm and the AP_5A-free AK_1 at $\delta_f = 7.865$ ppm can be clearly resolved. Simple line-shape simulations lead to the result that the off-rate of AP_5A under our experimental conditions is less than 1 s^{-1}. Qualitatively, the overall alteration of the protein spectrum is unlike either the change induced by AMP complexation or

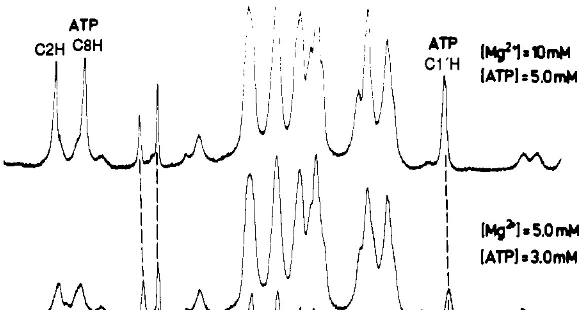

FIGURE 3: Same region of the spectrum as in Figure 2 at different ATP·Mg^{2+} concentrations. Experimental conditions as in Figure 2.

the change induced by ATP·Mg^{2+} complexation alone. In the adenosine resonance region between 5.6 and 8.8 ppm six newly emerging peaks can be observed clearly. These correspond to two sets of three resonances each from either adenosine moiety, namely, from C2-H and C8-H of the adenine rings and C1′-H of the sugar ring. The C1′-H resonance region around 5.8 ppm shows a broad singlet and a clearly resolved doublet peak from the bound AP_5A. Since these ribose C1′-H resonances cannot be attributed immediately to ATP·Mg^{2+} site and AMP site, respectively, we call the binding site giving rise to the lower field doublet resonance at δ = 6.09 ppm the "A-site" and the site corresponding to the higher field singlet resonance at δ = 5.91 ppm the "B-site".

(*A*) *NOESY Experiment.* The region of the resonances from protons of aromatic amino acid side chains of the NOESY spectrum of the AK_1·AP_5A·Mg^{2+} complex shows several intraprotein cross-peaks. In addition, cross-peaks between the lowest field proton resonance of AP_5A in the AP_5A·Mg^{2+}·AK_1 complex at δ = 9.1 ppm and the imidazole C2 proton of His^{36} can be observed (Figure 5). Also, a cross-peak clearly connects the C1′-H resonance of the ribose moiety of the AP_5A·Mg^{2+}·AK_1 A-site with the imidazole C2-H resonance of His^{36}. As the cross-peak intensities are dependent on the sixth power of the inverse proton–proton distance, they are extremely sensitive to the interproton distance. This means that the distance between the imidazole C2 proton and the adenine C2 proton is closer than 0.4 nm, which is a fairly widely accepted limit for the observability of an NOE in proteins (Wüthrich, 1986). The same is, of course, true for the distance between the C1′ proton of the A-site and the C2 proton of the imidazole of His^{36}. The only cross-peak which

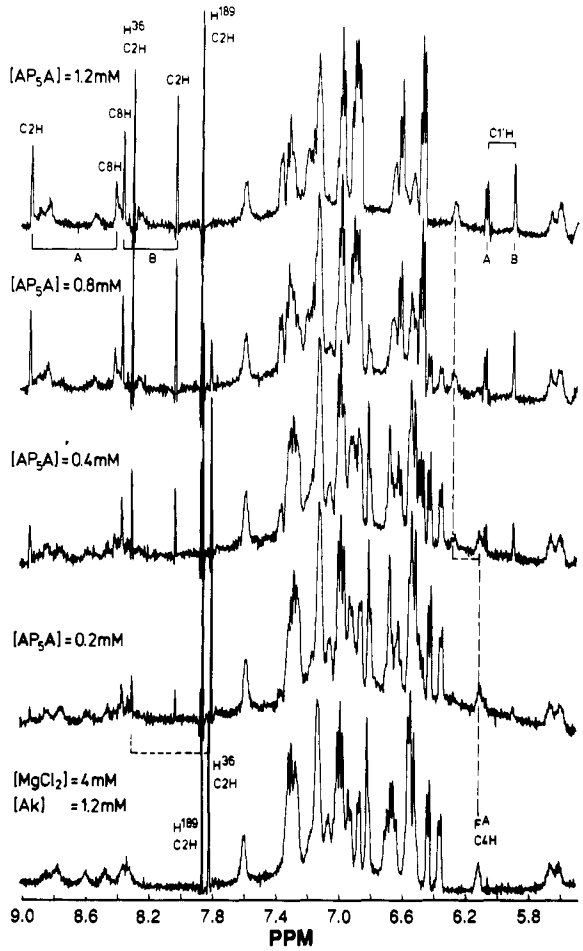

FIGURE 4: Same region of the spectrum as in Figure 2 at different AP_5A·Mg^{2+} concentrations. Experimental conditions as in Figure 2.

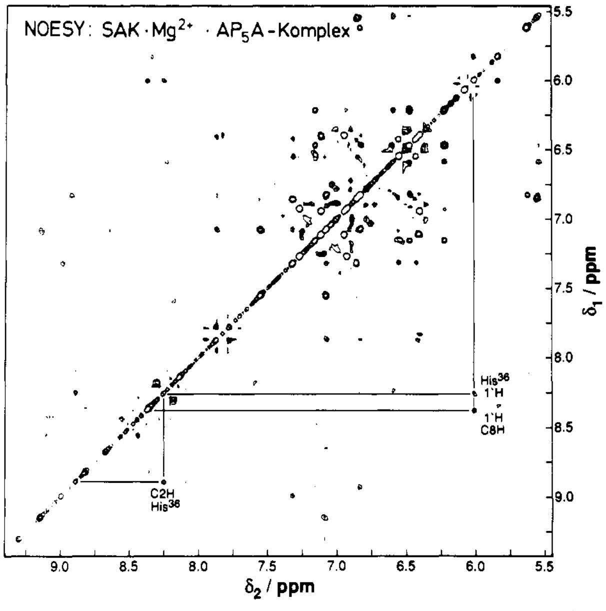

FIGURE 5: NOESY spectrum of the region of the aromatic residues and C2-H, C8-H, and C1′-H resonances of bound AP_5A·Mg^{2+}. The intramolecular AMP-site adenine C2-H–AMP-site ribose C1′-H cross-peak and the intermolecular cross-peaks His^{36} imidazole C2-H–AMP-site adenine C2-H and His^{36} imidazole–AMP-site ribose C1′-H are indicated by solid lines. Experimental conditions: T = 303 K; [AK] = [AP_5A] = 2.0 mM; phosphate buffer, 50 mM, pH 6.3; mixing time = 200 ms. The spectrum was symmetrized.

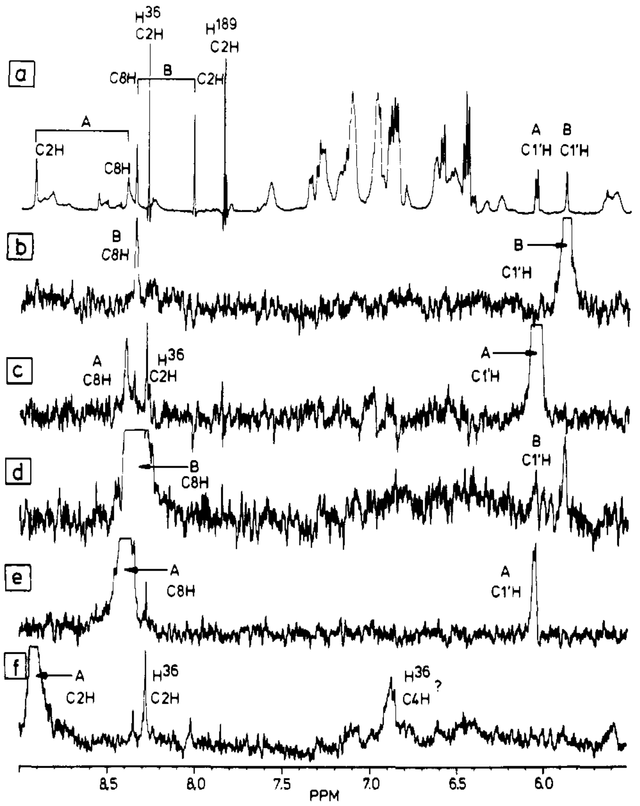

FIGURE 6: NOE difference spectra of the AK·AP$_5$A complex under the experimental conditions of Figure 4 and as described under Materials and Methods. Irradiation frequencies are indicated by arrows.

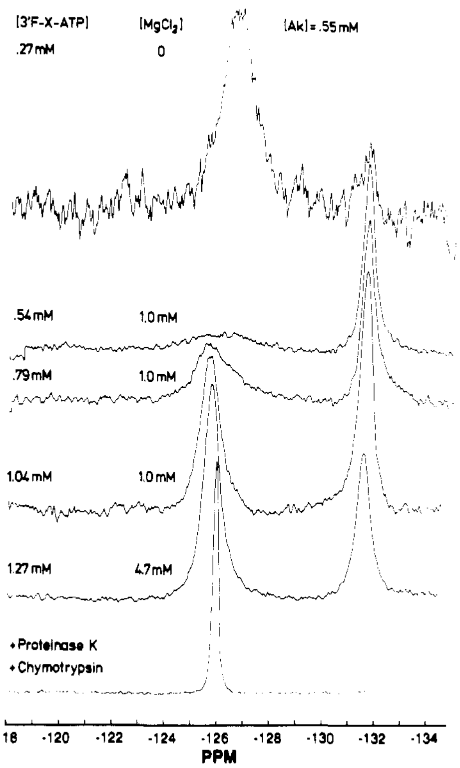

FIGURE 7: ^{19}F NMR spectra of a mixture of 3'-F-X-ATP, Mg^{2+}, and adenylate kinase. Experimental conditions: Hepes buffer, 50 mM, pH 8; $T = 278$ K; protein concentration = 0.55 mM; other conditions as indicated in the figure.

is intramolecular with respect to the bound dinucleotide which could be observed is the one between the adenine proton resonance at 8.42 ppm and the A-site ribose C1'-H. Thus, the lowest field resonance of the bound AP$_5$A at 8.96 ppm represents the A-site C2-H resonance, whereas the resonance at 8.42 ppm represents the A-site C8-H resonance, since the C8 proton is closer to C1'-H than the C2 proton of the same adenosine moiety in any nucleotide conformation.

(*B*) *One-Dimensional NOE Experiments.* To corroborate and extend the NOESY data, we also performed one-dimensional NMR experiments. In order to avoid spurious effects from unbound nucleotide, we did not use excess AP$_5$A but restricted our experiments to the stoichiometric complex. The NOE difference spectra—i.e., the spectra obtained by subtracting the spectra taken after on-resonance irradiation from the spectra taken after off-resonance irradiation—show several resonances from intra- as well as intermolecular dipolar interactions (Figure 6). All measured NOEs are negative, as expected for a molecular complex of this size at a resonance frequency of 500 MHz. From the intra AP$_5$A NOEs the connectivities of the resonances can be derived unequivocally (Figure 6a). Irradiation of the B-site ribose C1'-H resonance results in a decrease of the B-site adenine C8-H resonance (Figure 6b), whereas irradiation of the A-site ribose C1'-H resonance decreases the adenine C8-H resonance of the same site (Figure 6c). The reverse of these effects can also be observed (Figure 6d,e), so that the assignment of resonances is self-consistent. As expected from the NOESY experiments, a clear decrease of the imidazole C2-H resonance of His^{36} could be observed on irradiation of the A-site adenine C2-H (Figure 6f).

^{19}F NMR on the 3-Fluoro-3-deoxy-β-D-xylofuranosyl Nucleotide–AK$_1$ Complexes. The ^{19}F NMR spectrum of 3'-F-X-ATP in the presence of AK$_1$, but in the absence of added metal ions, shows essentially one broad peak at −125.7 ppm at an enzyme to 3'-F-X-ATP ratio of 2:1 (Figure 7, top trace). In addition, the spectrum shows a smaller peak at −131.6 ppm, the bigger peak probably being due to free 3'-F-X-ATP and the smaller one to the complex 3'-F-X-ATP·AK$_1$. The line widths of the resonances are likely to be mainly caused by chemical exchange between the free and the bound form. From the ratio of the two peaks and the known concentration of enzyme and 3'-F-X-ATP, the dissociation constant may be estimated to be around 5 mM. Addition of Mg^{2+} results in an increase of intensity of the ^{19}F resonance from the bound form, and even at a 3'-F-X-ATP to enzyme ratio of about 1:1 the bound form prevails by a large margin, corresponding to a decrease of the dissociation constant by at least 2 orders of magnitude induced by the presence of metal ions (Figure 7, second trace). Further addition of 3'-F-X-ATP then increases the intensity of the resonance originating from the free 3'-F-X-ATP·Mg^{2+}. The presence of metal ions does not change the ^{19}F chemical shift of the free and bound compounds within the limits of error imposed by the line width. Digestion of the adenylate kinase in the sample by incubation with a few milligrams of proteinase K and chymotrypsin at room temperature for several minutes leads, not unexpectedly, to the disappearance of the resonance of the bound 3'-F-X-ATP·Mg^{2+} (Figure 7, bottom trace). Removal of metal by addition of excess EDTA did change the chemical shift of the fluorine resonance slightly to −126.05 ppm.

Under the same conditions, addition of 0.27 mM 3'-F-X-AMP to 0.68 mM AK$_1$ resulted in the appearance of a single peak at −125.0 ppm (Figure 8, top trace). Addition of excess MgCl$_2$ did not alter the spectrum (Figure 8, second trace). Further addition of 3'-F-X-AMP brought about an upfield shift of the resonance toward the position of the free-nucleotide chemical shift. This shift was identical for 3'-F-X-AMP and the corresponding triphosphate, as can be seen in the spectrum

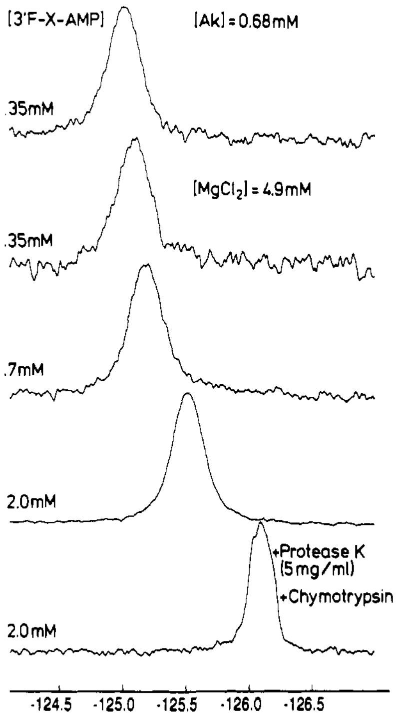

FIGURE 8: ^{19}F NMR spectra of a mixture of 3′-F-X-AMP, Mg^{2+}, and adenylate kinase. Experimental conditions: $T = 278$ K; Hepes buffer, 50 mM, pH 8; [AK] = 0.55 mM; other conditions as indicated in the figure.

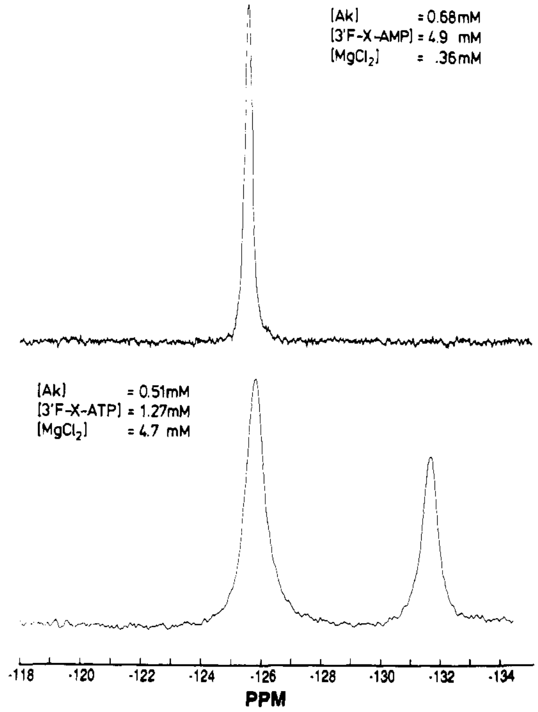

FIGURE 9: Comparison of the ^{19}F spectrum of a mixture of 3′-F-X-AMP, AK_1, and $MgCl_2$ with the ^{19}F spectrum of a mixture of 3′-F-X-ATP, AK_1, and $MgCl_2$. Experimental conditions: $T = 278$ K; Hepes buffer, 50 mM, pH 8.0; other conditions as indicated in the figure.

after AK_1 digestion by addition of protease K and chymotrypsin (Figure 8). Evaluation of the chemical shift in the free and bound states and the apparent dissociation constant yielded $\delta_f = -126.3$ ppm, $\delta_b = -123.7$ ppm, and $K_d = 7 \times 10^{-4}$ M. The off-rate is thus much greater than 1200 s^{-1}.

No fluorine resonance at the position of the 3′-F-X-ATP·Mg^{2+}·AK_1 resonance could be detected in the sample containing 3′-F-X-AMP, Mg^{2+}, and AK_1, even with a nearly 8-fold excess of nucleotide analogue over enzyme (Figure 9). On the other hand, the fluorine spectrum of the 3′-F-X-ATP·Mg^{2+}·AK_1 complex does not show a resonance at the position of the resonance of 3′-F-X-AMP·AK_1 in the presence of Mg^{2+} even at a 2.5-fold excess of 3′-F-X-ATP·Mg^{2+} over enzyme. This shows conclusively that 3′-F-X-AMP and 3′-F-X-ATP in the presence of Mg^{2+} do bind to the enzyme preferrentially (>95%) in different modes in the ribose 3′ region. As can be seen from the proton spectra of the complex AK_1·3′-F-X-AMP, the chemical shift value of the adenine C2-H of this compound is highly similar to the shift of the adenine C2-H of bound AMP, indicating a similar mode of binding around these protons (Auer et al., 1988).

DISCUSSION

From our fluorine NMR studies it is evident that the local environment of the sugar C3′-F position is different for the AK_1·3′-F-X-AMP and the AK_1·3′-F-X-ATP·Mg^{2+} complexes. The estimated dissociation constant of 5 mM for the AK_1·3′-F-ATP is much higher than the one measured by Hamada et al. (1979) for the AK_1·ATP complex with calf muscle and rabbit AK_1 (2.6×10^{-5} M). In contrast, our estimate of $K_d \leq 5 \times 10^{-5}$ M for the porcine AK_1·3′-F-X-ATP·Mg^{2+} complex is in good agreement with the number given by Hamada et al. (1979) for the rabbit and calf muscle AK_1·ATP·Mg^{2+} complexes. Thus, 3′-F-X-ATP·Mg^{2+} seems to be a good analogue for ATP·Mg^{2+} as far as binding to porcine AK_1 is concerned. In contrast, 3′-F-X-ATP is probably not an ideal substitute for ATP. The dissociation constant of the porcine AK_1·3′-F-X-AMP complex is an order of magnitude higher than the dissociation constant for the porcine AK_1·AMP complex ($K_d = 7 \times 10^{-4}$ M vs $K_d = 6.1 \times 10^{-5}$ M). Hamada et al. (1979) found a dissociation constant of $K_d \approx 10^{-4}$ M for the calf muscle and rabbit AK_1·AMP complex. The adenine C2-H resonance of the AK_1·3′-F-X-AMP complex also exhibits the peculiar downfield shift of the analogous resonance of the AK_1·AMP complex (Auer et al., unpublished results). This suggests that 3′-F-X-AMP binds to the same site in AK_1 as AMP does.

A downfield shift even more pronounced than that in the AK_1·AMP complex was also observed for the A-site adenine C2-H resonance of the AK_1·AP_5A·Mg^{2+} complex. This suggests that the adenosine binding to the A-site corresponds to the AMP binding at the AMP site. On the other hand, it is known from kinetic studies that either the AMP·Mg^{2+} complex or magnesium-free AMP is able to bind to the ATP·Mg^{2+} site (Rhoades & Lowenstein, 1968). Fry et al. (1985, 1987) and Smith and Mildvan (1982) observed a transferred NOE from the His^{36} imidazole C2-H to the adenine C2-H of excess ATP·Mg^{2+} with the porcine enzyme. They also observed an NOE from a His imidazole C2-H in the rabbit enzyme to the adenine C2-H of excess ATP·Mg^{2+}. Since there is much evidence for binding of ATP·Mg^{2+} to the "correct" site exclusively (Hamada et al., 1979), it would follow that the A-site of the AK_1·AP_5A·Mg^{2+} complex corresponds to the ATP·Mg^{2+} site.

On the basis of chemical shift arguments, adoption of the assignment of the A-site as representing the ATP·Mg^{2+} site would infer that AMP forms a binary complex with porcine AK_1 by binding to the ATP·Mg^{2+} site of the enzyme. So far, there is no experimental evidence for this assumption. In favor of partial binding of AMP to the ATP·Mg^{2+} site is the downfield shift of the C2-H of the imidazole ring of His^{36} on binding of either substrate, indicating similar local conformational changes of the protein induced on substrate binding. Unfortunately, the observation of the C2-H resonance of the bound ATP·Mg^{2+} is impaired by broadening of this peak in our experiments beyond detection in the stoichiometric complex, thus prohibiting the observation of a possible chemical shift change of this resonance on complexation.

The question whether the B-site in AK_1·AP_5A·Mg^{2+} represents the other substrate site in the active complex cannot be resolved easily. It is clear that the B-site is in fact a binding site on the protein, and does not represent an adenosine tumbling free in solution: The ribose C1′-H resonance of the B-site is shifted upfield from the unbound position and shows no resolved doublet splitting, indicating a structurally distorted sugar ring. In addition, the structural changes of the protein on AP_5A·Mg^{2+} binding as indicated by the changing NMR spectrum are different from the changes induced by binding of either substrate. Also, the off-rate of AK_1·AP_5A·Mg^{2+} is at least 3 orders of magnitude lower than the one for the AK_1·ATP·Mg^{2+} complexes determined from the NMR data. The ability to inhibit the porcine adenylate kinase reaction is higher for AP_5A than for either AP_4A or AP_6A (Feldhaus et al., 1975). Although other possibilities cannot be ruled out, this observation would fit the hypothesis that the AP_5A adenosines block both nucleotide sites by binding to them, whereas such binding is not possible for steric reasons for the two other bis(5′-adenosyl) phosphates.

As far as the determination of absolute distances from the NOE studies is concerned, all the observed NOEs are of nearly equal magnitude. In particular, the adenine C8-H to ribose C1′-H distance seems to be virtually identical for both sites. An NOE between either of the adenine C2-H and the corresponding C1′-H was not observed in our experiments. Earlier, the glycosydic bond of the AK_1-bound ATP·Mg^{2+} was suggested to be in anti conformation with an χ angle of 60–65° (Fry et al., 1985). In any case, the smallest C1′-H to C8-H distance possible is approximately 0.3 nm; the largest distance for which an NOE can be expected is approximately 0.4 nm (Wüthrich, 1986). A distance within this range can thus be also inferred between the adenine C2-H and the imidazole ring C2-H of His^{36} and between the ribose C1′-H and the imidazole ring C2-H of His^{36}, respectively.

Our observations are reconcilable at least partially with the results of earlier experiments on the binary nucleotide complexes in the presence of excess nucleotide: For example, no NOE could be observed with excess AMP over enzyme on irradiation of the His^{36} imidazole C2-H by Smith and Mildvan (1984), in accord with our results. In contrast, with a high excess of ATP·Mg^{2+} over enzyme a transferred NOE to the adenine C2-H was observed on irradiation of the His^{36} imidazole C2-H (Smith & Mildvan, 1984), a result we could not obtain under our conditions. Our failure to observe a substrate–protein NOE with the complex of AK and ATP·Mg^{2+} may be explained in many different ways, e.g., an exchange rate of the substrate leading to a correlation time unfavorable for observation of a substrate–protein NOE at 500 MHz.

What causes the large downfield shift of the C2-H resonance of the adenine of the A-site of AP_5A and of AMP on complexation? A straightforward explanation would be a hydrogen bond type interaction involving this proton. A different explanation could invoke a solvent effect on the chemical shift, as the ATP·Mg^{2+} adenine site is supposed to form a hydrophobic pocket in the protein structure.

The disagreement between the NMR results and the X-ray crystallographic location of the nucleotide binding sites as assumed to be mimicked by AP_5A in the yeast and *E. coli* enzymes (Egner et al., 1987; Müller & Schulz, 1988) could be caused by various effects:

First, only one nucleotide site could be occupied by AP_5A·Mg^{2+} in solution as well as in the crystals, and the other adenosine could be placed more or less randomly in the structure.

Second, the AP_5A·Mg^{2+} complex of the adenylate kinases could be different in solution and in the crystal.

Third, the long adenylate kinases with an additional loop region of about 30 amino acids (Schulz et al., 1986), which were so far studied exclusively by X-ray crystallography, could form an AP_5A·Mg^{2+} complex different from the corresponding complex of the short adenylate kinases, which were the exclusive subjects of NMR studies so far.

Under the adoption of the first hypothesis, the correct site in solution is most probably the one called A-site in our experiments. Neither of the adenines of AP_5A in the crystal structures binds to the region homologous to the His^{36} region of porcine AK_1. Thus, the adenosine moiety binding to a correct site would have to be different in solution and in the crystal. For example, one of the adenosines would represent the correct AMP site in the crystal, the other one binding unspecifically, and in solution the A-site would represent the ATP·Mg^{2+} site, the B-site representing an unspecific site.

Also, neither of the other suggestions can be excluded at present, and more work is needed on any one of the adenylate kinases whose crystal structure with bound AP_5A·Mg^{2+} is known.

We could show that neither of the substrates alone is able to induce the conformation of the enzyme which it adopts in the AP_5A·Mg^{2+} complex. The latter result, although not entirely unexpected, should be kept in mind for future structural work on the subject.

ACKNOWLEDGMENTS

We thank Prof. Dr. K. C. Holmes for encouragement and support and Birgit Brandmeier, Marija Isakov, and Sabine Zimmermann for skilled technical assistance.

REFERENCES

Auer, M., Rösch, P., Sczakiel, G., & Goody, R. S. (1988) *Nucleosides Nucleotides* (in press).

Barzu, O., & Michelson, S. (1983) *FEBS Lett. 153*, 280–284.

Bax, A., & Davis, D. G. (1985) *J. Magn. Reson. 65*, 355–360.

Berghäuser, J., & Schirmer, R. H. (1978) *Biochim. Biophys. Acta 537*, 454–463.

Egner, U., Tomasselli, A. G., & Schulz, G. E. (1987) *J. Mol. Biol. 195*, 649–658.

Ehresman, B., Imbault, P., & Weil, J. H. (1973) *Anal. Biochem. 54*, 454–463.

Feldhaus, P., Fröhlich, T., Goody, R. S., Isakov, M., & Schirmer, R. H. (1975) *Eur. J. Biochem. 57*, 197–204.

Fry, D. C., Kuby, S. A., & Mildvan, A. S. (1985) *Biochemistry 24*, 4680–4694.

Fry, D. C., Kuby, S. A., & Mildvan, A. S. (1987) *Biochemistry 26*, 1645–1655.

Fry, D. C., Byler, D. M., Susi, H., Brown, E. M., Kuby, S. A., & Mildvan, A. S. (1988) *Biochemistry 27*, 3588–3598.

Hamada, M., Palmierei, R., Russell, G. A., & Kuby, S. A. (1979) *Arch. Biochem. Biophys. 195(1)*, 155–177.

Kalbitzer, H. R., Marquetant, R., Rösch, P., & Schirmer, R. H. (1982) *Eur. J. Biochem. 126*, 531–536.

Klaus, W., Scharf, M., & Rösch, P. (1988) *Biochemistry 27*, 5407–5411.

Lienhard, G. E., & Secemski, I. I. (1973) *J. Biol. Chem. 248*, 1121–1123.

Marion, D., & Wüthrich, K. (1983) *Biochem. Biophys. Res. Commun. 113*, 967–974.

McDonald, G. G., Cohn, M., & Noda, L. (1975) *J. Biol. Chem. 250*, 6947–6954.

Müller, C. W., & Schulz, G. E. (1988) *J. Mol. Biol. 202*, 909–912.

Nageswara Rao, B. D., Cohn, M., & Noda, L. (1978) *J. Biol. Chem. 253*, 1149–1158.

Noda, L. (1973) *Enzymes (3rd Ed.) 8*, 279–305.

Rance, M., & Wright, P. E. (1986) *J. Magn. Reson. 66*, 372–378.

Rösch, P., & Gross, K. H. (1985) *J. Mol. Biol. 182*, 341–345.

Schulz, G. E., Elzinga, M., Marx, F., & Schirmer, R. H. (1974) *Nature 250*, 120–123.

Schulz, G. E., Schiltz, E., Tomasselli, A. G., Frank, R., Brune, M., Wittinghofer, A., & Schirmer, R. H. (1986) *Eur. J. Biochem. 161*, 127–132.

Shyy, Y.-I., Tian, G., & Tsai, M.-D. (1987) *Biochemistry 26*, 6411–6415.

Smith, G. M., & Mildvan, A. S. (1982) *Biochemistry 21*, 6119–6123.

Tomasselli, A. G., & Noda, L. H. (1980) *Eur. J. Biochem. 103*, 481–491.

Wüthrich, K. (1986) *NMR of Proteins and Nucleic Acids*, Wiley, New York.

---

^{31}P NMR Visibility and Characterization of Rat Liver Mitochondrial Matrix Adenine Nucleotides[†]

Susan M. Hutson,[*,‡,§] Deborah Berkich,[‡] Gerald D. Williams,[∥] Kathryn F. LaNoue,[‡] and Richard W. Briggs[∥,⊥,#]

Department of Physiology, Department of Biological Chemistry, and Radiology NMR Laboratory, The Milton S. Hershey Medical Center of the Pennsylvania State University, Hershey, Pennsylvania 17033

Received September 7, 1988; Revised Manuscript Received February 6, 1989

ABSTRACT: Compartmentation and NMR visibility of mitochondrial adenine nucleotides were quantitated in isolated rat liver mitochondria respiring on succinate and glutamate in vitro at 8 and 25 °C. Intra- and extramitochondrial nucleotides were discriminated by adding the chelator *trans*-1,2-diaminocyclohexane-*N,N,N′,N′*-tetraacetic acid (CDTA). T_1 values of about 0.2–0.3 s for magnesium-bound matrix nucleotides were determined. Adenine nucleotide T_1 values were influenced by the ionic environment; only magnesium-free ATP T_1's were affected by temperature. Intra- and extramitochondrial adenine nucleotide ratios were varied in ATP-loaded mitochondria with added ATP and phosphate using the mitochondrial inhibitors oligomycin and carboxyatractyloside, and adenine nucleotides were quantitated by using NMR and enzymatic analysis. There was good agreement between matrix ATP concentrations (magnesium-bound ATP) calculated by using NMR and standard biochemical techniques. Although matrix ADP could be detected by NMR, it was difficult to quantitate accurately by NMR. The data indicate that mitochondrial ATP is NMR-visible in isolated mitochondria in vitro.

Discrepancies between estimates of adenine nucleotide metabolites determined by phosphorus-31 nuclear magnetic resonance (^{31}P NMR)[1] spectroscopy and estimates determined by enzymatic analysis have suggested the existence of NMR-invisible pools within the cell (Freeman et al., 1983; Iles et al., 1985; Stubbs et al., 1984; Murphy et al., 1988). The largest inconsistencies have been observed with ADP. In muscle, this has been attributed to the binding of ADP to actin, which results in a broadening of the ADP resonances. On the other hand, in the liver and kidney, which do not contain significant amounts of actin, it has been suggested that it is the mitochondrial pool of ADP which is not observable (Iles et al., 1985; Freeman et al., 1983). Good agreement has been found between ATP measured by ^{31}P NMR in vivo or in perfused livers and ATP determined in acid extracts of liver tissue (Iles et al., 1985; Stubbs et al., 1984; Cunningham et al., 1986; Desmoulin et al., 1987). In fact, the liver β-ATP signal was used as a calibration standard by Iles et al. (1985). However, differences between ATP levels measured by ^{31}P NMR and enzymatic assays of perchloric acid extracts of freeze-clamped livers subjected to ischemia have been reported recently (Murphy et al., 1988). On the basis of published values (Aw et al., 1987) for ATP compartmentation in isolated hepatocytes subjected to hypoxia, Murphy et al. (1988) concluded the differences could be attributed to invisibility of ATP in the mitochondrial pool. NMR-silent ATP has also been reported in the perfused heart (Takami et al., 1988; Neely et al., 1988).

In the original NMR studies of isolated mitochondria, Ogawa et al. (1978), Shen et al. (1980), and Ogawa and Lee (1982) concluded that mitochondrial adenine nucleotides were

---

[†] This work was supported by Grants DK-34738 (S.M.H.), HL-36948 and HL-18708 (K.F.L.), CA-39627 (R.W.B.), and P41-RR02278 (R.W.B. and principal investigator, K. N. Scott) from the National Institutes of Health, U.S. Public Health Service.

[*] Author to whom correspondence should be addressed.

[‡] Department of Physiology.

[§] Present address: Department of Biochemistry, Wake Forest University, Bowman Gray School of Medicine, 300 South Hawthorne Rd., Winston-Salem, NC 27103.

[∥] Radiology NMR Laboratory.

[⊥] Present address: Department of Radiology, University of Florida College of Medicine, Box J-374, J. H. Miller Health Center, Gainesville, FL 32610.

[#] Department of Biological Chemistry.

[1] Abbreviations: ^{31}P NMR, phosphorus-31 nuclear magnetic resonance; T_1, spin–lattice relaxation time; CDTA, *trans*-1,2-diaminocyclohexane-*N,N,N′,N′*-tetraacetic acid; EDTA, ethylenediaminetetraacetic acid; Mops, 4-morpholinepropanesulfonic acid; Pipes, 1,4-piperazinediethanesulfonic acid; FCCP, carbonyl cyanide *p*-(trifluoromethoxy)phenylhydrazone.

0006-2960/89/0428-4325$01.50/0